

BackPlay: Plug-in Look-Back Self-Correction for Diffusion Language Models*

Liming Liu, Binxuan Huang, Zixuan Zhang, Xin Liu, Bing Yin, Tuo Zhao

February 5, 2026

Abstract

Diffusion Language Models (DLMs) have achieved significant efficiency gains by generating multiple tokens in parallel. However, this parallel sampling approach, especially when using fewer inference steps, will introduce strong dependency errors and cause quality to deteriorate rapidly as the generation step size grows. As a result, reliable self-correction becomes essential for maintaining high-quality multi-token generation. To address this, we propose BackPlay, a Plug-in framework that enables DLMs to perform autonomous self-correction. BackPlay freezes the parameters of a finetuned DLM to preserve its peak performance while training a specialized correction head added on top of the model. This head is trained specifically on the errors generated by the frozen and well-optimized model, enabling it to capture the model’s intrinsic error distribution. To further enhance the head’s effectiveness, we introduce Look-back Correction, a training mechanism that empowers the head to leverage current contextual information to supervise and rectify mistakes made in earlier generation steps. During inference, our framework enables the model to jointly generate and revise tokens, effectively mitigating error accumulation. Experiments on mathematical reasoning and code generation benchmarks demonstrate that our approach substantially reduces quality degradation in large-step generation, allowing DLMs to achieve both high speed and strong output fidelity.

1 Introduction

Diffusion Language Models (DLMs) have emerged as a powerful alternative to autoregressive (AR) models for language generation, offering substantial speedups through parallel decoding (Sahoo et al., 2024; Nie et al., 2024; Ye et al., 2025; Zhu et al., 2025). Unlike AR models that generate tokens sequentially, DLMs start from a fully masked sequence and iteratively reveal tokens through a denoising process, producing multiple tokens simultaneously at each step. This parallel generation enables substantially faster inference while achieving competitive performance across reasoning, coding, and planning tasks (Nie et al., 2025; Ye et al., 2025; Zhu et al., 2025).

The efficiency gains of parallel generation come with inherent challenges. As DLMs generate multiple tokens in the same iteration, particularly under a small number of denoising steps, they

*Amazon. Correspondence to 11ming@amazon.com

are susceptible to dependency errors across positions (Liu et al., 2024; Xu et al., 2024; Kang et al., 2025). Critically, errors introduced in early denoising steps persist and propagate through subsequent iterations, degrading generation quality. This vulnerability naturally motivates the need for self-correction mechanisms that can detect and rectify erroneous predictions during inference.

Existing approaches to self-correction in DLMs typically perform refinement by selectively remasking previously generated tokens and regenerating them under the current partially denoised context. Several recent works explore training-free strategies (Wang et al., 2025; Zhao et al., 2024; Peng et al., 2025). For instance, Wang et al. (2025) employ random remasking, which can be inefficient when sequences are long and errors are sparse. Zhao et al. (2024) and Peng et al. (2025) use model-derived confidence scores to guide token selection, but these scores lack explicit training or calibration to predict token correctness, limiting their reliability and systematic improvement. More recently, trainable correction modules have been proposed (Huang et al., 2025; Kim et al., 2025), typically by jointly optimizing both the DLM and a self-correction head with a multi-objective loss.

While these joint training approaches have demonstrated effectiveness, we identify two critical limitations. First, simultaneously optimizing generation and correction objectives can degrade the base model’s generative capability, revealing an inherent trade-off between generation fidelity and correction capacity. Second, methods requiring concurrent training of both components are difficult to integrate with DLMs that have undergone extensive post-training or instruction tuning, as they necessitate modifying well-optimized parameters. This substantially limits their applicability in production environments where pretrained models cannot be easily retrained.

1.1 Our Contribution

In this work, we propose BackPlay: Plug-in Look-Back Self-Correction framework, which allows DLMs to self-correct reliably without compromising their core generative fidelity. Our contributions are threefold:

- We decouple the optimization of the DLM from the correction head. By freezing the fine-tuned DLM and training only the auxiliary head, we preserve DLM’s original generative quality while significantly enhancing training efficiency. This approach provides a lightweight, Plug-in solution that avoids the high computational costs of full-parameter updates.
- We propose Look-back Correction training recipe: we simulate a “hindsight” scenario by embedding early-stage errors generated from highly corrupted states into the expanded context of later stages. This intentional temporal mismatch can train the correction head to leverage late-arriving context to identify historical mistakes that typically persist during inference.
- We demonstrate that BackPlay provides a robust and efficient self-correction framework, achieving superior performance across complex DLM generation tasks.

1.2 Concurrent Work

At the end of our project, we notice the concurrent work PRISM (Kim et al., 2025) released. PRISM shares similar motivation with us, but diverges in optimization strategy and training distribution modeling. We discuss the detailed difference in Section 2.3, Section 3.1 and Section 3.2.

2 Preliminaries and Related Works

2.1 Diffusion Language Models (DLMs)

Diffusion Language Models (DLMs) (Nie et al., 2024, 2025; Ye et al., 2025; Zhu et al., 2025) are built on the foundations of discrete diffusion models (Austin et al., 2021; Lou et al., 2023; He et al., 2023; Sahoo et al., 2024; Gat et al., 2024; Shi et al., 2024). They consist of a forward corruption process that replaces tokens with a special mask token \mathbb{M} and a reverse process that restores masked tokens given the current partially observed sequence. We present the training procedure to learn this reverse process and the inference procedure to generate new sequences.

Forward process. DLMs generate discrete sequences by iteratively denoising partially masked inputs. Let $\mathbf{x}_0 \in \mathcal{V}^L$ be a length- L clean sequence sampled from dataset \mathcal{D} with vocabulary \mathcal{V} . \mathbb{M} is the mask token used as noise. For time $t \in [0, 1]$, the corrupted sequence $\mathbf{x}_t \in (\mathcal{V} \cup \{\mathbb{M}\})^L$ is sampled by independently masking each position:

$$q_{t|0}(\mathbf{x}_t | \mathbf{x}_0) = \prod_{i=1}^L q_{t|0}(x_t^i | x_0^i),$$

$$q_{t|0}(x_t^i | x_0^i) = \begin{cases} \alpha_t, & x_t^i = x_0^i, \\ 1 - \alpha_t, & x_t^i = \mathbb{M}. \end{cases}$$

We follow common practice in DLMs to adopt the linear schedule $\alpha_t = 1 - t$. As t increases from 0 to 1, more tokens are masked, until at $t = 1$ the sequence is fully masked.

Reverse process and Training. The reverse process is defined by transition distributions $\{q_{s|t}(\mathbf{x}_s | \mathbf{x}_t)\}_{0 \leq s < t \leq 1}$ that keep unmasked tokens fixed and update masked positions:

$$q_{s|t}(x_s^i | \mathbf{x}_t) = \begin{cases} \mathbb{I}(x_s^i = x_t^i), & x_t^i \neq \mathbb{M}, \\ \frac{s}{t} (x_s^i = \mathbb{M}) + \frac{t-s}{t} q_{0|t}(x_s^i | \mathbf{x}_t), & x_t^i = \mathbb{M}, \end{cases}$$

where \mathbb{I} is the indicator function and $q_{0|t}(\cdot | \mathbf{x}_t)$ is the posterior distribution over clean tokens. We parameterize this with a model $p_\theta(\mathbf{x}_0 | \mathbf{x}_t)$ trained to predict original tokens from masked inputs by minimizing the demasking loss:

$$\mathcal{L}_{\text{Demask}}(\theta) = \mathbb{E} \left[\frac{1}{t} \sum_{i: x_t^i = \mathbb{M}} -\log p_\theta(x_0^i | \mathbf{x}_t) \right], \quad (2.1)$$

where the expectation is based on

$$t \sim \text{Unif}[0, 1], \mathbf{x}_0 \sim \mathcal{D}, \mathbf{x}_t \sim q_{t|0}(\cdot | \mathbf{x}_0)$$

Inference. At generation time, we use the trained model to iteratively unmask a sequence starting from a fully masked sequence $\mathbf{x}_1 = (\mathbb{M}, \dots, \mathbb{M})$. The process proceeds over a decreasing sequence of time steps $t_0 = 1 > \dots > t_N = 0$. At each step ℓ , given the partially masked sequence \mathbf{x}_{t_ℓ} , the transition to $\mathbf{x}_{t_{\ell+1}}$ involves two steps:

1. **Selection:** Identify a subset $\mathcal{S}_\ell \subseteq \{i : \mathbf{x}_{t_\ell}^i = \mathbb{M}\}$ of masked tokens to unmask. Common selection strategies include uniform selecting a fixed fraction of remaining masks (Austin et al., 2021), and confidence-based selecting the most confident positions under p_θ (Nie et al., 2025).
2. **Prediction:** For all positions $i \in \mathcal{S}_\ell$ simultaneously, sample the token values \mathbf{x}_0^i from the model’s predicted distribution $p_\theta(x_0^i | \mathbf{x}_{t_\ell})$. These positions are generated in parallel via a single forward pass $p_\theta(x_0 | \mathbf{x}_{t_\ell})$.

2.2 Self-Correction of DLMs

The parallel update is the main source of speedup in DLMs inference. However, DLMs are trained to learn per-position posteriors of the form $p(x_0^{(i)} | \mathbf{x}_t)$ rather than the full joint conditional distribution $p(\mathbf{x}_0 | \mathbf{x}_t) = p(x_0^{(1:N)} | \mathbf{x}_t)$. Consequently, different positions are denoised largely independently, and cross-token dependencies can be systematically violated during parallel decoding (Liu et al., 2024; Xu et al., 2024; Kang et al., 2025).

This limitation motivate the need for self-correction. Several training-free methods have attempted remasking or refinement strategies (Zhao et al., 2024; Wang et al., 2025; Peng et al., 2025), but these often rely on heuristic quality estimates and cannot be explicitly optimized or explained, which limits their accuracy and general applicability. To further enhance the self-correction capability of DLMs, recent works like Huang et al. (2025) and Kim et al. (2025) propose trainable self-correction methods.

Trainable self-correction methods augment the base model with a correction function $\mathbf{g}_{\theta, \phi}(\mathbf{z}_t)$ that predicts per-token correctness probabilities for a sequence \mathbf{z}_t , where θ denotes DLM parameters and ϕ denotes auxiliary correction head parameters. This correction function allows the model to identify and remask potentially erroneous tokens for regeneration in later stages. The correction function is $\mathbf{g}_{\theta, \phi}$ trained using Binary Cross-Entropy (BCE) loss to perform per-token binary classification:

$$\mathcal{L}_{Err}(\theta, \phi) = \mathbb{E} \left[\sum_i \text{BCE}(\mathbf{g}_{\theta, \phi}^i(\mathbf{z}_t), \mathbb{I}[z_t^i = x_0^i]) \right], \quad (2.2)$$

where the expectation is based on

$$t \sim \text{Unif}[0, 1], \mathbf{x}_0 \sim \mathcal{D}, \mathbf{z}_t,$$

The key design choice is constructing training sequences \mathbf{z}_t with realistic mixtures of correct and incorrect tokens. Prior methods such as RemeDi (Huang et al., 2025) and PRISM (Kim et al., 2025) start with a corrupted sequence $\mathbf{x}_t \sim q_{t|0}(\mathbf{x}_0)$ and introduce “artifact” tokens $\mathbf{y} \sim P_{\text{artifact}}$ at selected

positions $\mathcal{M} \subseteq \{i : \mathbf{x}_t^i \neq \mathbb{M}\}$. The training sequence \mathbf{z}_t is generated by

$$\mathbf{z}_t = \text{replace}(\mathbf{x}_t, \mathbf{y}, \mathcal{M}), \quad \text{where}$$

$$[\text{replace}(\mathbf{x}_t, \mathbf{y}, \mathcal{M})]_i = \begin{cases} y_t^i, & \text{if } i \in \mathcal{M}, \\ x_t^i, & \text{otherwise.} \end{cases}$$

The artifact distribution P_{artifact} and the selection of positions \mathcal{M} together determine which error types the correction head learns to detect, making them crucial design choices. RemeDi specifies P_{artifact} as uniform distribution $\text{Unif}(\mathcal{V}^L)$, which fails to account for the structured, context-dependent errors typical of language models. PRISM generates artifacts from the model’s own predictions: given a time step size Δt , it samples a slightly more corrupted state $\mathbf{x}_{t+\Delta t}$ to predict \mathbf{y} :

$$\mathbf{x}_{t+\Delta t} \sim q_{t+\Delta t|0,t}(\cdot | \mathbf{x}_0, \mathbf{x}_t), \quad \mathbf{y} \sim p_\theta(\mathbf{x}_0 | \mathbf{x}_{t+\Delta t}),$$

and selects \mathcal{M} from positions that are masked in $\mathbf{x}_{t+\Delta t}$ but unmasked in \mathbf{x}_t . Here \mathcal{M} contains $\lceil L \cdot \Delta t \rceil$ positions to simulate the transition during reverse process from $\mathbf{x}_{t+\Delta t}$ to \mathbf{x}_t . \mathcal{M} can be selected either randomly or based on the confidence of $p_\theta(\mathbf{x}_0 | \mathbf{x}_{t+\Delta t})$.

Both methods jointly optimize the base model and correction head parameters:

$$\mathcal{L}(\theta, \phi) = \mathcal{L}_{\text{Demask}}(\theta) + \gamma \times L_{\text{Err}}(\theta, \phi), \quad (2.3)$$

where γ is a hyperparameter that balances the demasking and error detection objectives.

2.3 Limitations

Current trainable self-correction frameworks, such as RemeDi (Huang et al., 2025) and PRISM (Kim et al., 2025), integrate error detection into the Diffusion Language Model (DLM) pipeline. However, these approaches suffer from three primary bottlenecks that hinder their effectiveness in real-world generation tasks.

Capacity Trade-off in Optimization. Existing methods typically optimize the base model parameters θ and the correction head ϕ simultaneously using a weighted objective in Equation (2.3). This joint optimization creates a capacity trade-off. The model must balance the task of high-quality token generation with the task of error identification. As shown in Table 1, this dual-objective training can lead to negative interference and degrade the DLM’s generative ability. Moreover, finding the optimal γ to mitigate this interference remains a non-trivial challenge.

Artifact Distribution Misalignment. The effectiveness of correction head $\mathbf{g}_{\theta, \phi}$ is tied to how well the artifact distribution P_{artifact} mirrors the actual errors encountered during inference. However, both RemeDi and PRISM introduce a training-deployment gap. Because θ is optimized alongside ϕ , the correction head in PRISM primarily learns to identify errors produced by a under-optimized model. These errors often reflect underfitting, and may deviate from the structural biases and dependency errors for a fully converged model. Consequently, the correction head remains misaligned with the high-fidelity outputs it is expected to monitor during inference.

Lack of Look-back Capability. In discrete diffusion, a token generated at an early denoising step may appear locally plausible given the sparse context available. As more tokens are unmasked

in subsequent steps, the expanded context provides the evidence needed to reveal these early decisions as globally erroneous. PRISM attempt to predict errors immediately after a single step of generation, which is an excessively difficult task because the available context is still sparse. More importantly, this creates a misalignment with the inference process. For a robust correction head, the ability to utilize the continually expanding context of later steps during inference to “look back” is more vital than immediate detection. This provides the head with richer information and multiple opportunities during the denoising process to identify an earlier error as the sequence evolves.

3 Method

3.1 Decoupled Self-Correction Training

To address the limitations of *Capacity Trade-off in Optimization and Artifact Distribution Misalignment* discussed in Section 2.3, BackPlay treats the finetuned DLM as a frozen feature backbone and appends a Plug-in lightweight correction head to identify the generation errors.

Given that DLM parameters θ^* have already undergone sufficient Supervised Fine-Tuning (SFT), we freeze θ^* to preserve the integrity of its generative priors, and introduce a correction head ϕ implemented as a shallow Transformer. To leverage the rich contextual representations already captured by θ^* , the head ϕ operates on the hidden states from the penultimate layer. Formally, let L denote the total number of layers in the frozen DLM. The correction function $\mathbf{g}_{\theta^*, \phi}$ is defined as:

$$\mathbf{g}_{\theta^*, \phi}(\mathbf{z}_t) = \phi(\mathbf{h}^{L-1}), \quad (3.1)$$

where \mathbf{h}^{L-1} represents the hidden states extracted during the forward pass of $p_{\theta^*}(\mathbf{x}_0 | \mathbf{z}_t)$. This design ensures that the correction head functions as a non-intrusive probe, utilizing high-level semantic features already computed by the backbone to identify misalignments.

We utilize the frozen weights θ^* to generate artifact-containing training samples \mathbf{z}_t via Look-back Correction (detailed in Section 3.2). Correction head ϕ is optimized using a Binary Cross-Entropy (BCE) loss:

$$\mathcal{L}(\phi) = \mathbb{E} \left[\sum_i \text{BCE}(\mathbf{g}_{\theta^*, \phi}(\mathbf{z}_t)_i, \mathbb{I}[z_t^i = x_0^i]) \right] \quad (3.2)$$

where the expectation is based on $t \sim \mathcal{U}(0, 1)$, $\mathbf{x}_0 \sim \mathcal{D}$, \mathbf{z}_t . Our framework offers *several advantages*:

Preservation of Generative Fidelity: By freezing the optimized weights θ^* , we prevent any degradation of the generative performance and eliminate sensitivity to the balancing hyperparameter γ in Equation (2.3). Our framework is compatible with DLMs that have already undergone extensive post-training, as it removes the risk of eroding established capabilities during the self-correction training phase.

Accurate Error Alignment: Training ϕ on the artifacts of the well-optimized θ^* ensures the correction head learns the specific, structured error patterns. Because ϕ is tasked with identifying the errors generated by θ^* during inference, our training recipe aligns the training distribution

with actual deployment scenarios. This strategy effectively addresses the distribution misalignment challenges typically found in joint optimization.

Training Efficiency: Since θ^* is frozen, we eliminate the need for backbone backpropagation and the storage of full DLM forward activations. Unlike LoRA-based methods used in PRISM that require complete backward passes for adapter gradients, our framework only maintains optimizer states for the lightweight head ϕ , significantly reducing GPU memory overhead and accelerating training.

Inference Efficiency: By utilizing the penultimate hidden states \mathbf{h}^{L-1} already computed during the DLM’s forward pass, the head identifies errors with minimal additional FLOPs, ensuring high-speed generation.

3.2 Look-back Correction

To further address the limitation of *Lack of Look-back Capability* in Section 2.3, we propose Look-back Correction (LBC). Recall that θ^* denotes the frozen DLM parameters and Δt is the time step size. For any given time step t and $\mathbf{x}_t \sim q_{t|0}(\cdot|\mathbf{x}_0)$, we sample $t' \sim \mathcal{U}[\Delta t, 1 - t]$, generate a more corrupted state $\mathbf{x}_{t+t'} \sim q_{t+t'|0,t}(\cdot|\mathbf{x}_0, \mathbf{x}_t)$, and generate the artifact tokens \mathbf{y} using the frozen DLM:

$$\mathbf{y} \sim p_{\theta^*}(\mathbf{x}_0|\mathbf{x}_{t+t'}).$$

We select a subset $\mathcal{M} \subseteq \{i : \mathbf{x}_{t+t'}^i = \mathbb{M}\}$ with $|\mathcal{M}| = \lceil L \cdot \Delta t \rceil$, and construct the training sequence using $\mathbf{z}_t = \text{replace}(\mathbf{x}_t, \mathbf{y}, \mathcal{M})$. To emulate the actual inference process, \mathcal{M} is selected following the confidence-based strategy introduced by Nie et al. (2025). Specifically, we construct \mathcal{M} by identifying the masked positions where $p_{\theta^*}(\mathbf{x}_0|\mathbf{x}_{t+t'})$ exhibits the highest confidence. We formalize LBC method in Algorithm 2.

Intuitively, \mathbf{z}_t is constructed to imitate the scenario where historical errors persist into later stages of the denoising process. We simulate a trajectory where the model initially generates predictions \mathbf{y} for positions in \mathcal{M} from an earlier, more uncertain state $\mathbf{x}_{t+t'}$. We then assume that all subsequent denoising steps between $t+t'$ and t are performed perfectly, thereby retaining the ground-truth context in \mathbf{x}_t for all positions outside \mathcal{M} .

By embedding these early-stage errors from $p_{\theta^*}(\mathbf{x}_0|\mathbf{x}_{t+t'})$ into the late-stage correct context of \mathbf{x}_t , we create a synthetic state \mathbf{z}_t that mirrors a common inference flaw: incorrect tokens that were plausible in a more corrupted state but are revealed as errors by the richer context available at time t . This forces the correction head ϕ to learn “hindsight” error detection by cross-referencing suspicious tokens with their surrounding refined context.

3.3 Inference with Adaptive Remasking

After training stage, we deploy the trained model with parameters (θ^*, ϕ^*) using an inference procedure that corrects errors during generation. Unlike standard DLM generation, which simply applies $p_{\theta^*}(\mathbf{x}_0|\mathbf{x}_t)$ at each denoising step, our approach strategically remasks wrong tokens identified by the correction function $\mathbf{g}_{\theta^*, \phi^*}$, allowing the model to regenerate them with richer context in subsequent steps.

During remasking process, the correction function $\mathbf{g}_{\theta^*, \phi^*}$ evaluates the sequence \mathbf{x}_t to estimate the error probability P_{error} for each generated token. We define a remasking budget K to target the most unreliable tokens predicted by $\mathbf{g}_{\theta^*, \phi^*}$; specifically, $\mathcal{M}_{\text{remask}}$ includes the indices with the Top- K highest error probabilities. We further gate this process with a threshold τ . Tokens are only remasked if their error probability exceeds τ , preventing unconfident perturbations when the correction head deems the current generation to be possibly correct.

Algorithm 1 Dynamic Self-Correction Inference

Require: Generative model θ^* , Tokens generated per step k , Generation length L , Correction head ϕ^* , Remasking budget K , Confidence threshold τ , Self-correction stride d , Block buffer capacity B .

```

1:  $\Delta t \leftarrow \frac{k}{L}$ ,  $T \leftarrow \lceil \frac{L}{k} \rceil$ ,  $t \leftarrow 1$ ,  $N \leftarrow 0$ ,
    $\mathbf{x}_1 \leftarrow [\text{MASK}]^L$ ,  $\mathcal{H}_{\text{block}} \leftarrow \emptyset$  (queue)
2: while  $t > 0$  do
3:    $t_{\text{new}} \leftarrow \max\{t - \Delta t, 0\}$ ,  $x_{t_{\text{new}}} \leftarrow x_t$ 
    $\mathcal{M} \leftarrow \{i \mid x_t^{(i)} = [\text{MASK}]\}$ ,  $\mathcal{M}_{\text{remask}} \leftarrow \emptyset$ 
4:    $P_{\text{demask}} \leftarrow p_{\theta^*}(\mathbf{x}_0 \mid \mathbf{x}_t)$ 
5:    $\mathcal{I} \leftarrow \text{arg-top-}k_{i \in \mathcal{M}} \left( P_{\text{demask}}^{(i)} \right)$ 
6:   Sample  $\mathbf{x}_{t_{\text{new}}}[i] \sim P_{\text{demask}}[i]$  for all  $i \in \mathcal{I}$ 
7:   if  $N \bmod d = 0$  then
8:      $P_{\text{error}} \leftarrow \mathbf{g}_{\theta^*, \phi^*}(\mathbf{x}_t)$ 
9:      $\mathcal{M}_{\text{candid}} \leftarrow \text{arg-top-}K(P_{\text{error}})$ 
10:    for index  $i$  in  $\mathcal{M}_{\text{candid}}$  do
11:      if  $P_{\text{error}}(i) > \tau$  and  $i \notin \mathcal{H}_{\text{block}}$  then
12:        Add  $i$  to  $\mathcal{M}_{\text{remask}}$ 
13:      end if
14:    end for
15:    for index  $i$  in  $\mathcal{M}_{\text{remask}}$  do
16:       $\mathbf{x}_{t_{\text{new}}}[i] \leftarrow [\text{MASK}]$ 
17:      if  $|\mathcal{H}_{\text{block}}| \geq B$  then
18:        Remove the oldest element from  $\mathcal{H}_{\text{block}}$ 
19:      end if
20:      Append  $i$  to  $\mathcal{H}_{\text{block}}$ 
21:    end for
22:  end if
23:   $t \leftarrow t_{\text{new}}$ 
24:   $t \leftarrow t + \frac{|\mathcal{M}_{\text{remask}}|}{L}$ ,  $N \leftarrow N + 1$ 
25: end while

```

After remasking, the generation timeline will then rollback to adapt to the new number of [MASK] tokens:

$$t_{\text{back}} = t + \frac{|\mathcal{M}_{\text{remask}}|}{L} \quad (3.3)$$

where L is the generation length. The model can then regenerate these positions later using richer context. Furthermore, to prevent frequent remasking from harming sequence completeness, we employ a periodic remasking strategy controlled by a stride d . The remasking process is triggered only at specific denoising steps N where $N \pmod d = 0$.

Anti-Repetitive Correction Policy: In practice, we found an important issue in iterative self-correction is the risk of oscillatory error correction, where a token is repeatedly predicted as an error and subsequently re-generated identically by the DLM. This wastes remasking capacity and stalls the generation process. To address this, we maintain a memory $\mathcal{H}_{\text{block}}$ of the indices that have been remasked in the recent few steps. Tokens whose indices are present in $\mathcal{H}_{\text{block}}$ are temporarily prohibited from being remasked again. This strategy ensures that the self-correction mechanism prioritizes exploration of new error tokens, preventing cycles and optimizing the utilization of the limited remasking budget.

We summarize our inference techniques and show the specific algorithm in Algorithm 1.

4 Experiments

4.1 SMDM Fine-Tuning Setting

We conduct experiments under two settings: In the first setting we use SMDM 1B (Nie et al., 2024) as the base model and the augmented math data Deng et al. (2023) as the dataset. In the second setting, we use LLaDA 8B Base (Nie et al., 2025) as the base model. We choose OpencodeInstruct (Ahmad et al., 2025) as the training dataset on coding, and OpenmathInstruct (Toshniwal et al., 2024) as the training dataset on math reasoning.

4.2 Experiments on SMDM 1B

Following the setting in SMDM (Nie et al., 2024), we use the 1B pretrained model from SMDM as base model and implement standard SFT on the augmented data (Deng et al., 2023) to get the finetuned model θ^* . Based on θ^* , we apply our training recipe in Section 3.1 and Section 3.2 to get the correction head ϕ^* . We use the zero-shot accuracy (Pass@1) on GSM8k (Cobbe et al., 2021) as test metric.

We also conduct ablation study on joint optimization. We use Equation (2.3) as loss function and train the model parameters θ and correction head ϕ simultaneously. We name the final parameters after joint optimization as $(\theta + \phi)^*$.

4.2.1 Implementation Details

Following the architecture proposed in Section 3.1, we use the output hidden state of the 19th transformer block of SMDM 1B model (20 layers in total) as the input to the correction head ϕ . The correction head ϕ is a 2 layers transformer. For both our framework and joint optimization, we generate the training sequence \mathbf{z}_t using LBC method in Section 3.2, so the only difference between our BackPlay and joint optimization is whether train the DLM θ and the correction head ϕ simultaneously or separately.

During inference, without self-correction (i.e., remask) applied, all models will use the confidence based strategy in Algorithm 3, proposed by [Nie et al. \(2025\)](#). With self-correction applied, all models will use dynamic Self-Correction Inference in Algorithm 1. The choice of hyperparameters are shown in Section [C](#).

4.2.2 Results on Generative Fidelity

Table 1: GSM8K test accuracy. Joint optimization underperforms SFT baseline without remask applied during inference. With remask applied, it still underperforms our BackPlay framework.

Model	Acc.(No Remask)	Acc.(Remask)
SFT (Baseline, θ^*)	61.33	–
Joint Optim ($\theta + \phi$) [*]	60.56	62.62
BackPlay (θ^*, ϕ^*)	61.33	63.46

We show the results on GSM8K in Table 1. The results highlight the capability trade-offs in joint optimization and the advantage of our framework:

Generative Degradation with Joint Optimization: When the correction head is trained simultaneously with the base DLM (Joint Optimization), the model’s intrinsic generative fidelity suffers. The accuracy without applying remasking drops to 60.56%, indicating that the dual objective optimization has compromised the model’s generative capability. In contrast, we freeze θ at θ^* before training ϕ , successfully preserves the generative integrity of the base model. Its performance without remasking remains at the SFT peak level (61.33%).

Notable improvement with Correction: When the self-correction mechanism (via remasking) is applied, both methods improve significantly over the SFT_{Base}. Furthermore, our framework consistently outperforms Joint Optimization (63.46% vs. 62.62%). This demonstrates that starting from an optimally tuned θ^* and training the correction head on a more aligned error distribution yields a more powerful and accurate self-correction mechanism.

4.3 Experiments on LLaDA 8B

To further evaluate the efficiency and performance of our framework, we conduct experiments across Coding and Math Reasoning on LLaDA 8B ([Nie et al., 2025](#)). For Coding experiments, we use LLaDA 8B Base as base model and implement standard SFT on the first 500,000 samples from OpenCodeInstruct ([Ahmad et al., 2025](#)) to get the finetuned model θ^* , and apply our method to train the correction head ϕ^* on the same 500,000 samples. Similarly, for Math reasoning experiments, we still use LLaDA 8B Base as base model and implement standard SFT on the first 500,000 samples from OpenMathInstruct ([Toshniwal et al., 2024](#)) and apply our method to train the corresponding correction head ϕ^* on the same samples.

4.3.1 Implementation Details

Our implementation details on LLaDA are similar to that in Section 4.2.1. We use output hidden state of the 31st transformer block of LLaDA 8B model (32 blocks in total) as the input to the correction head ϕ . The correction head ϕ is a 3 layers transformer.

For inference, SFT baseline model θ^* is using the confidence based strategy proposed in Nie et al. (2025) (Algorithm 3). Our model (θ^*, ϕ^*) is using dynamic self-correction inference shown in Algorithm 1. The choice of hyperparameters is shown in Section E. We employ semi-autoregressive generation protocol proposed in LLaDA (Nie et al., 2025): a block length of 32 tokens and a maximum total generation length of 1024 tokens. After the generation of each block, we implement **early stopping** strategy, which means we will stop the generation if we detect the “End-of-Sequence” token [EoS] in this block.

We find that semi-autoregressive generation with early stopping strategy already brings substantial sampling speedups. Our generation length is 1024; therefore, if one token is generated per iteration, it would require 1024 iterations. However, simply applying the semi-autoregressive strategy together with early stopping, LLaDA only needs about 100–200 iterations on MBPP and GSM8k, which corresponds to more than a 5 \times speedup compared to the standard approach. To ensure a fair comparison, we apply this strategy to both the baseline and our method.

4.3.2 Coding Experiments

We evaluate the performance of our framework against the SFT baseline on the MBPP and HumanEval benchmarks. We report Acc (Pass@1) under zero-shot setting to measure generative quality, and Iter_{avg}, the average number of sampling steps (equivalently, the average number of model forward passes) to measure inference efficiency.

Across all methods, increasing the number of tokens generated per sampling step reduces Iter_{avg} but also decreases accuracy, reflecting the accuracy–efficiency trade-off reported in LLaDA (Nie et al., 2025).

Table 2: Comparative results with SFT baseline on MBPP.

Method	Tokens / Step	Acc(%)	Iter _{avg}
SFT (Baseline)	1	39.8	119.4
	2	35.6	59.3
	3	30.4	44.3
	4	24.6	30.0
Our Method	1	40.2	134.0
	2	40.0	69.6
	3	35.8	45.6
	4	33.8	35.9

Table 2 summarizes the comparative results on the MBPP benchmark. Table 3 summarizes the comparative results on the HumanEval benchmark. Our goal is to demonstrate that by introducing

Table 3: Comparative results with SFT on HumanEval.

Method	Tokens / Step	Acc(%)	Iter _{avg}
SFT (Baseline)	1	35.98	131.0
	2	28.66	67.1
	3	24.39	41.5
	4	20.73	29.2
Our Method	1	36.59	138.6
	2	33.54	71.1
	3	33.29	41.5
	4	27.44	35.5

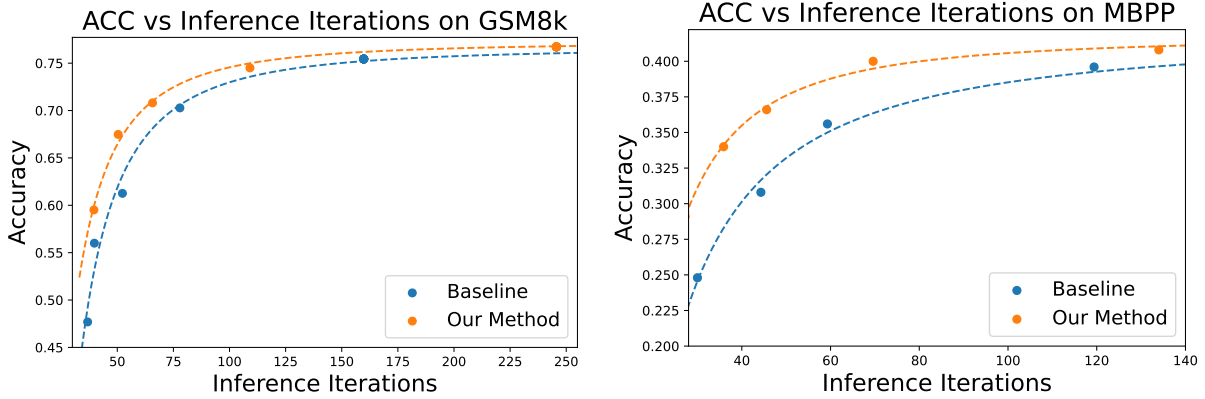


Figure 1: The accuracy vs. iterations comparison between our method and baseline SFT on GSM8k and MBPP. Data is from Table 2 and Table 4. Our methods is Pareto better than baseline.

our self-correction framework, even under more aggressive multi-token generation, DLM is able to maintain high generative quality while benefiting from reduced inference iterations, thereby achieving a Pareto-superior accuracy–efficiency trade-off. For example, on MBPP benchmark, with 2-tokens per step our approach reached higher accuracy than baseline with 1-token per step. More importantly, it significantly reduced the inference iterations by 41.7%. We also plot the relationship between average iteration and accuracy in Figure 1 to demonstrate how our method expands the Pareto frontier compared to the baseline and other methods.

4.3.3 Mathematical Reasoning Experiments

We evaluate the zero-shot accuracy (Pass @1) on GSM8k and Math (Hendrycks et al., 2021). Table 4 summarizes the comparative results on GSM8K. Table 5 summarizes the comparative results on Math. Introducing our self-correction framework to DLM still achieves a Pareto-superior accuracy–efficiency trade-off against the baseline. For example, on GSM8K benchmark, with 3-tokens per step our approach reached higher accuracy than baseline with 2-token per step. It significantly reduced the inference iterations by 15.7%. We also plotted the relationship between

average iteration and accuracy in Figure 1.

Table 4: Comparative results with SFT baseline on GSM8K.

Method	Tokens / Step	Acc(%)	Iter _{avg}
SFT (Baseline)	1	75.44	159.8
	2	70.28	77.9
	3	61.26	52.3
	4	56.18	39.8
	5	47.69	36.8
Our Method	1	76.72	245.6
	2	74.30	109.1
	3	70.81	65.7
	4	67.48	50.4
	5	59.51	39.6

Table 5: Comparative results with SFT baseline on Math.

Method	Tokens / Step	Acc(%)	Iter _{avg}
SFT (Baseline)	1	34.2	190.5
	2	31.6	85.3
	3	28.4	61.1
	4	22.4	47.1
Our Method	1	36.2	324.42
	2	34.0	127.9
	3	33.6	75.4
	4	28.4	56.1

4.4 Ablation on Artifact Distribution

To further illustrate how the quality of artifact distribution impacts the capability of the correction head, we conduct the following ablation study: while maintaining the training recipe in Section 3.1, we replaced the P_{artifact} in Look-back Correction (Section 3.2) with uniform distribution, consistent with that used in RemeDi. With all other training and inference methods to be the same, we re-train the correction head and re-evaluate the test accuracy on MBPP and GSM8k under the setting of LLaDA 8B discussed in Section 4.3.2 and Section 4.3.3. See the results in Table 6 and Table 7. We plot the results in Figure 2 to show that our method is Pareto better.

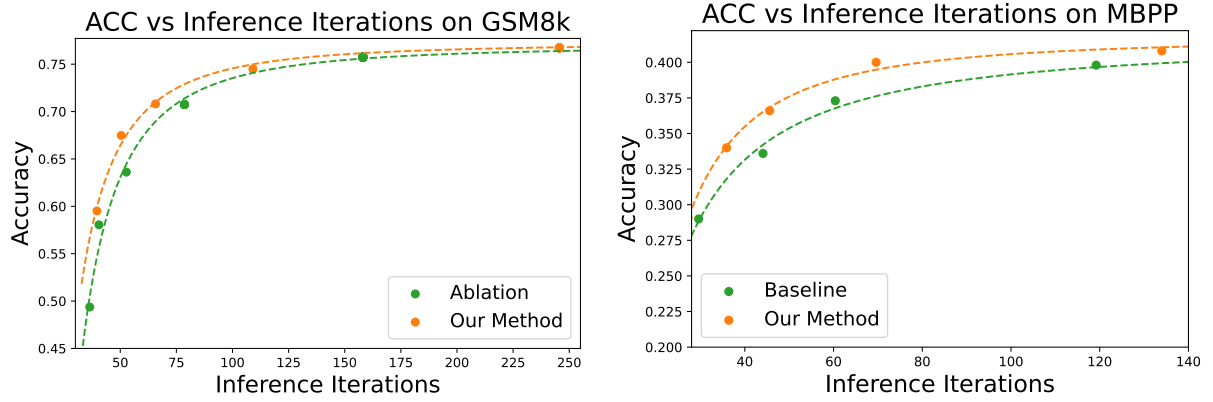


Figure 2: The accuracy vs. iterations comparison between our method and the ablation method in Section 4.4 on GSM8k and MBPP. Data is from Table 6 and Table 7. Our methods is Pareto better than the ablation method.

Table 6: Comparative results with ablation method on MBPP.

Method	Tokens / Step	Acc(%)	Iter _{avg}
Ablation	1	40.0	119.2
	2	37.6	60.4
	3	33.8	44.1
	4	29.8	29.6
Our Method	1	40.2	134.0
	2	40.0	69.6
	3	35.8	45.6
	4	33.8	35.9

Table 7: Comparative results with ablation method on the GSM8K.

Method	Tokens / Step	Acc(%)	Iter _{avg}
Ablation	1	75.74	158.1
	2	70.74	78.6
	3	63.61	52.7
	4	58.38	40.5
	5	49.37	36.4
Our Method	1	76.72	245.6
	2	74.30	109.1
	3	70.81	65.7
	4	67.48	50.4
	5	59.51	39.6

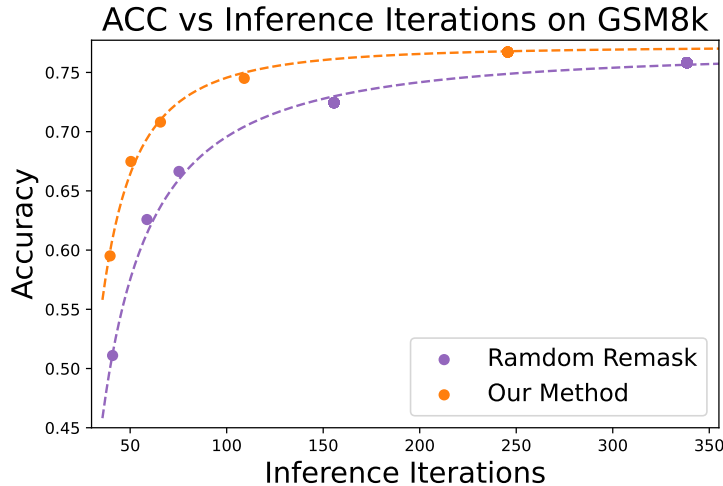


Figure 3: The accuracy vs. iterations comparison between our method and randomly remasking method on GSM8k. Data is from Table 8. Our methods is Pareto better than the ablation method.

4.5 Comparison with Random Remasking

We compare our method with random remasking methods proposed in [Wang et al. \(2025\)](#). Since we use semi-autoregressive method to generate the response and use early stopping strategy to save the inference iterations, there isn't a standard time schedule for the decoding process as in [Wang et al. \(2025\)](#). Instead, we simply adjust P_{error} in dynamic self-correction inference (Algorithm 1) to be independent random probability in $U[0, 1]$ assigned for all tokens that have been demasked. Thus in every remasking iteration the remasking tokens are randomly selected.

Table 8: Comparative results with random remasking method on GSM8K.

Method	Tokens / Step	Acc(%)	Iter _{avg}
Random Remask	1	75.82	338.4
	2	71.95	155.6
	3	66.64	75.3
	4	63.08	58.7
	5	51.10	40.9
Our Method	1	76.72	245.6
	2	74.30	109.1
	3	70.81	65.7
	4	67.48	50.4
	5	59.51	39.6

We found that while random remasking can improve the final accuracy beyond SFT baseline, it cannot precisely target incorrect tokens. Many correct tokens are unnecessarily masked and must be regenerated in subsequent sampling iterations. Because each step produces a fixed number of tokens, this inefficiency increases the total number of decoding iterations substantially.

We compare our BackPlay framework with such random remasking method on GSM8K, as shown in Table 8. We also plot the results in Figure 3 to show that our method is Pareto better than randomly remasking.

5 Conclusion

In this paper, we propose BackPlay, a novel self-correction framework for Diffusion Language Models (DLMs). BackPlay decouples the training of the DLM and the correction head: we freeze the optimized DLM and train only the correction head to address the errors produced by finetuned DLM. This design preserves the DLM’s generative capability while aligning the correction head’s training distribution with the error patterns it will encounter at inference time. Furthermore, we introduce Look-back correction, which allows the model to exploit additional future context to uncover and fix errors that may have gone unnoticed in earlier steps. Finally, we develop a dynamic self-correction inference procedure that integrates the DLM with the optimized correction head, substantially improving generation quality across benchmarks. Our results demonstrate that structured self-correction is an effective way to elevate the quality of parallel text generation.

References

AHMAD, W. U., FICEK, A., SAMADI, M., HUANG, J., NOROOZI, V., MAJUMDAR, S. and GINSBURG, B. (2025). Opencodeinstruct: A large-scale instruction tuning dataset for code llms. *arXiv preprint arXiv:2504.04030*.

AUSTIN, J., JOHNSON, D. D., HO, J., TARLOW, D. and VAN DEN BERG, R. (2021). Structured denoising diffusion models in discrete state-spaces. *Advances in neural information processing systems*, **34** 17981–17993.

COBBE, K., KOSARAJU, V., BAVARIAN, M., CHEN, M., JUN, H., KAISER, L., PLAPPERT, M., TWOREK, J., HILTON, J., NAKANO, R. ET AL. (2021). Training verifiers to solve math word problems. *arXiv preprint arXiv:2110.14168*.

DENG, Y., PRASAD, K., FERNANDEZ, R., SMOLENSKY, P., CHAUDHARY, V. and SHIEBER, S. (2023). Implicit chain of thought reasoning via knowledge distillation. *arXiv preprint arXiv:2311.01460*.

GAT, I., REMEZ, T., SHAUL, N., KREUK, F., CHEN, R. T., SYNNAEVE, G., ADI, Y. and LIPMAN, Y. (2024). Discrete flow matching. *Advances in Neural Information Processing Systems*, **37** 133345–133385.

HE, Z., SUN, T., TANG, Q., WANG, K., HUANG, X.-J. and QIU, X. (2023). Diffusionbert: Improving generative masked language models with diffusion models. In *Proceedings of the 61st annual meeting of the association for computational linguistics (volume 1: Long papers)*.

HENDRYCKS, D., BURNS, C., KADAVATH, S., ARORA, A., BASART, S., TANG, E., SONG, D. and STEINHARDT, J. (2021). Measuring mathematical problem solving with the math dataset. *arXiv preprint arXiv:2103.03874*.

HUANG, Z., WANG, Y., CHEN, Z. and QI, G.-J. (2025). Don't settle too early: Self-reflective remasking for diffusion language models. *arXiv preprint arXiv:2509.23653*.

KANG, W., GALIM, K., OH, S., LEE, M., ZENG, Y., ZHANG, S., HOOPER, C., HU, Y., KOO, H. I., CHO, N. I. ET AL. (2025). Parallelbench: Understanding the trade-offs of parallel decoding in diffusion llms. *arXiv preprint arXiv:2510.04767*.

KIM, J., KIM, S., LEE, T., PAN, D. Z., KIM, H., KAKADE, S. and CHEN, S. (2025). Fine-tuning masked diffusion for provable self-correction. *arXiv preprint arXiv:2510.01384*.

LIU, A., BROADRICK, O., NIEPERT, M. and BROECK, G. V. D. (2024). Discrete copula diffusion. *arXiv preprint arXiv:2410.01949*.

LOU, A., MENG, C. and ERMON, S. (2023). Discrete diffusion modeling by estimating the ratios of the data distribution. *arXiv preprint arXiv:2310.16834*.

NIE, S., ZHU, F., DU, C., PANG, T., LIU, Q., ZENG, G., LIN, M. and LI, C. (2024). Scaling up masked diffusion models on text. *arXiv preprint arXiv:2410.18514*.

NIE, S., ZHU, F., YOU, Z., ZHANG, X., OU, J., HU, J., ZHOU, J., LIN, Y., WEN, J.-R. and LI, C. (2025). Large language diffusion models. *arXiv preprint arXiv:2502.09992*.

PENG, F. Z., BEZEMEK, Z., PATEL, S., RECTOR-BROOKS, J., YAO, S., BOSE, A. J., TONG, A. and CHATTERJEE, P. (2025). Path planning for masked diffusion model sampling. *arXiv preprint arXiv:2502.03540*.

SAHOO, S., ARRIOLA, M., SCHIFF, Y., GOKASLAN, A., MARROQUIN, E., CHIU, J., RUSH, A. and KULESHOV, V. (2024). Simple and effective masked diffusion language models. *Advances in Neural Information Processing Systems*, **37** 130136–130184.

SHI, J., HAN, K., WANG, Z., DOUCET, A. and TITSIAS, M. (2024). Simplified and generalized masked diffusion for discrete data. *Advances in neural information processing systems*, **37** 103131–103167.

TOSHNIWAL, S., DU, W., MOSHKOV, I., KISACANIN, B., AYRAPETYAN, A. and GITMAN, I. (2024). Openmathinstruct-2: Accelerating ai for math with massive open-source instruction data. *arXiv preprint arXiv:2410.01560*.

TOUVRON, H., MARTIN, L., STONE, K., ALBERT, P., ALMAHAI, A., BABAEI, Y., BASHLYKOV, N., BATRA, S., BHARGAVA, P., BHOSALE, S. ET AL. (2023). Llama 2: Open foundation and fine-tuned chat models. *arXiv preprint arXiv:2307.09288*.

WANG, G., SCHIFF, Y., SAHOO, S. S. and KULESHOV, V. (2025). Remasking discrete diffusion models with inference-time scaling. *arXiv preprint arXiv:2503.00307*.

XU, M., GEFFNER, T., KREIS, K., NIE, W., XU, Y., LESKOVEC, J., ERMON, S. and VAHDAT, A. (2024). Energy-based diffusion language models for text generation. *arXiv preprint arXiv:2410.21357*.

YE, J., XIE, Z., ZHENG, L., GAO, J., WU, Z., JIANG, X., LI, Z. and KONG, L. (2025). Dream 7b: Diffusion large language models. *arXiv preprint arXiv:2508.15487*.

ZHAO, Y., SHI, J., CHEN, F., DRUCKMANN, S., MACKEY, L. and LINDERMAN, S. (2024). Informed correctors for discrete diffusion models. *arXiv preprint arXiv:2407.21243*.

ZHU, F., WANG, R., NIE, S., ZHANG, X., WU, C., HU, J., ZHOU, J., CHEN, J., LIN, Y., WEN, J.-R. ET AL. (2025). Llada 1.5: Variance-reduced preference optimization for large language diffusion models. *arXiv preprint arXiv:2505.19223*.

A Implementation Details of LBC

We summarize the Look-back Correction algorithm in Algorithm 2.

Algorithm 2 Look-back Correction (LBC) Training Recipe

- 1: **Input:** Clean data \mathbf{x}_0 , frozen SFT parameters θ^* , Step size Δt , sequence length L
- 2: Sample time step $t \sim \mathcal{U}[0, 1]$
- 3: Sample state $\mathbf{x}_t \sim q_{t|0}(\cdot | \mathbf{x}_0)$
- 4: Sample forward interval $t' \sim \mathcal{U}[\Delta t, 1 - t]$
- 5: Sample more corrupted state $\mathbf{x}_{t+t'} \sim q_{t+t'|0,t}(\cdot | \mathbf{x}_0, \mathbf{x}_t)$
- 6: Generate artifact sequence: $\mathbf{y} \sim p_{\theta^*}(\mathbf{x}_0 | \mathbf{x}_{t+t'})$
- 7: Calculate subset size: $k = \lceil L \cdot \Delta t \rceil$
- 8: Identify masked indices: $\mathcal{I}_{mask} = \{i : \mathbf{x}_{t+t'}^i = [\text{MASK}]\}$
- 9: Select top- k confident indices from \mathcal{I}_{mask} :

$$\mathcal{M} = \arg\text{-top-}k_{i \in \mathcal{I}_{mask}} (p_{\theta^*}(\mathbf{x}_0^i | \mathbf{x}_{t+t'}^i))$$
- 10: Construct training sequence: $\mathbf{z}_t = \text{replace}(\mathbf{x}_t, \mathbf{y}, \mathcal{M})$
- 11: **Return:** Training pair $(\mathbf{z}_t, \mathbf{x}_0)$

B Training Details on SMDM 1B

For the SFT stage, we use the 1B pretrained model from SMDM (Nie et al., 2024) as base model. Following the setting in SMDM, we train the model on the augmented data (Deng et al., 2023). We first train the model for 40 epochs following (Nie et al., 2024). Then we try to train for 80 epochs and find it still increases the test accuracy on GSM8k. Thus we fixed the setting to train the model 80 epochs on the augmented data (Deng et al., 2023). The training details are shown in Table 9.

For the training of self-correction head, we train the model on the same augmented data (Deng et al., 2023) for 20 epochs. The training details is summarized in Table 10. For joint optimization, we share the same hyperparameters as SFT in Table 9. We tune the trade-off hyperparameter γ in $\{0.01, 0.1, 0.5\}$ and select the best result.

C Inference Details on SMDM 1B

For inference without remasking, following the setting in SMDM and LLaDA (Nie et al., 2025), we use the confidence based strategy as shown in Algorithm 3. Every iteration we choose the top- k positions where the model have the largest confidence and demask these positions. For inference with remasking, we use the dynamic self-correction inference method in Algorithm 1 for both BackPlay framework and the joint optimization models. Details are summarized in Table 11.

Table 9: Config of SFT for SMDM 1B

Base Model	
Architecture	SMDM (Nie et al., 2024)
Parameters	1028M
Tokenizer	LLaMA2 Tokenizer (Touvron et al., 2023)
Training	
Sequence Length	256
Optimizer	AdamW
Learning Rate	2×10^{-4}
Weight Decay	0.1
Global Batch Size	256
β_1	0.9
β_2	0.95
Warmup Ratio	0.01
Learning Rate Schedule	cosine

Algorithm 3 Confidence based inference strategy from LLaDA ([Nie et al., 2025](#))

Require: Generative model θ^* , Tokens generated per step k , Generation Length L .

- 1: $\Delta t \leftarrow \frac{k}{L}$, $\mathbf{x}_1 \leftarrow [\text{MASK}]^L$, $t \leftarrow 1$
- 2: **while** $t > 0$ **do**
- 3: $t_{\text{new}} \leftarrow \max\{t - \Delta t, 0\}$, $x_{t_{\text{new}}} \leftarrow x_t$, $\mathcal{M} \leftarrow \{i \mid x_t^{(i)} = [\text{MASK}]\}$
- 4: $P_{\text{demask}} \leftarrow p_{\theta^*}(\mathbf{x}_0 \mid \mathbf{x}_t)$
- 5: $\mathcal{I} \leftarrow \text{arg-top-}k_{i \in \mathcal{M}}(P_{\text{demask}}^{(i)})$
- 6: Sample $\mathbf{x}_{t_{\text{new}}}[i] \sim P_{\text{demask}}[i]$ for all $i \in \mathcal{I}$
- 7: $t \leftarrow t_{\text{new}}$
- 8: **end while**

D Training Details on LLaDA 8B

D.1 Supervised Finetuning (SFT)

our SFT for LLaDA 8B Base basically follows the method proposed in LLaDA ([Nie et al., 2025](#)). We set the maximum length to be 1024 and use the special token “End-of-Sentence”([EoS]) to pad all the data to be the maximum length.

In LLaDA ([Nie et al., 2025](#)), these padding [EoS] tokens are treated as normal tokens, which means that they will be also randomly masked with the same probability as tokens in the response. However, if the majority data are much shorter than the max length, there will be too many [EoS] tokens in the final padded data, and the model learn to predict [EoS] with a high probability. The result is that the model will tend to end the response early even though the response is not completed. We note that LLaDA ([Nie et al., 2025](#)) also report this issue for their finetuned instruct

Table 10: Training config of SMDM 1B self-correction head

Model	
Architecture	2-layers transformer
Parameters	90M
Training	
Step Size Δt in LBC	$\frac{1}{32}$
Sequence Length	256
Optimizer	AdamW
Learning Rate	2×10^{-3}
Weight Decay	0.1
Global Batch Size	256
β_1	0.9
β_2	0.95
Warmup Ratio	0.01
Learning Rate Schedule	cosine

Table 11: Inference config of SMDM 1B

Inference	
Generation Length	256
Tokens per step k	2
Dynamic Self-correction	
Confidence threshold τ	0.75
Max remask tokens K	2
Self-correction stride d	4
Block buffer B	4

model in their github.

To address this issue, we make a small but effective modification during the SFT stage. We still treat the first 16 [EoS] tokens as normal tokens, which means these tokens may still be masked. For the other [EoS] padding tokens, we just keep them to be unmasked. This method will effectively constrain the number of [EoS] tokens that need to be predicted in the SFT data. We found that this method effectively address the issue that the model tends to predict [EoS] token and end the response.

Finally we use the standard SFT loss for diffusion LLM as in Equation (2.1) to train the base model. We train LLaDA 8B Base on the first 500,000 samples from Opencodeinstruct (Ahmad et al., 2025) for coding experiments in Section 4.3.2 and the first 500,000 samples from Openmathinstruct (Toshniwal et al., 2024) for math reasoning experiments in Section 4.3.3 respectively and test the finetuned model on Coding and Math benchmarks correspondingly. The hyperparameters are summarized in Table 12.

D.2 Training of the self-correction head

The training of the self-correction head is after the SFT stage, and the parameter of the DLM θ^* is well optimized. Then we use a transformer block ϕ with two layers to be self correction head. The correction head ϕ takes the output of the 31st layer of the DLM to be the input, and it outputs a probability to predict whether the token is true or wrong. The correction head ϕ has only about 600M parameters, so the training of ϕ is very light weight. The training method is introduced in Section 3.1 and Section 3.2. Training dataset for head ϕ is completely same as that for θ^* , which is introduced in Section D.1. Same as the trick in Section D.1, we treat the first 16 [EoS] tokens

Table 12: Config for SFT of LLaDA 8B

Base Model	
Architecture	LLaDA Base (Nie et al., 2025)
Parameters	8B
Tokenizer	LLaDA Tokenizer (Nie et al., 2025)
Training	
Sequence Length	1024
Optimizer	AdamW
Learning Rate	2.5×10^{-5}
Weight Decay	0.1
Global Batch Size	256
β_1	0.9
β_2	0.95
Warmup Ratio	0.01
Learning Rate Schedule	cosine

as normal tokens, and keep the other [EoS] padding tokens to be unmasked during the generate process of \mathbf{z}_t in Equation (3.2). The training hyperparameters are summarized in Table 13.

D.3 Training details of ablation study

For the ablation study conducted in Section 4.4, we only need to re-train the self-correction head on the new training data. We keep all the training and inference hyperparaters to be the same as that in Section D.2.

E Inference Details on LLaDA 8B

For the SFT baseline, we still use the confidence based strategy from LLaDA, as shown in Algorithm 3. For model trained with our BackPlay framework, we use the dynamic self-correction inference in Algorithm 1. Tokens per step k are swiped to compare the accuracy-efficiency trade-off, as discussed in the main text and shown in different result tables. Other hyperparameters of inference are summarized in Table 14. For the randomly remasking experiments in Section 4.5, we keep all the hyperparameters same as that of dynamic self-correction inference. We just adjust P_{error} in dynamic self-correction inference (Algorithm 1) to be independent random probability in $U[0, 1]$ assigned for all tokens

Table 13: Training config of LLaDA 8B self-correction head

Model	
Architecture	3-layers transformer
Parameters	600M
Training	
Step Size Δt in LBC	$\frac{1}{64}$
Sequence Length	1024
Optimizer	AdamW
Learning Rate	5×10^{-4}
Weight Decay	0.1
Global Batch Size	256
β_1	0.9
β_2	0.95
Warmup Ratio	0.01
Learning Rate Schedule	cosine

Table 14: Inference config of LLaDA 8B

Inference	
Generation Length	1024
Tokens per step k	-
Dynamic Self-correction	
Confidence threshold τ	0.75
Max remask tokens K	2
Self-correction stride d	4
Block buffer B	4